Iranian Journal of Basic Medical Sciences
ijbms.mums.ac.ir

Exploring the renoprotective effects of umbelliferone in rats subjected to ischemia/reperfusion injury

Omer Faruk Baser [1], Ali Guraslan [2], Bengul Ozdemir Sarikaya [2], Selina Aksak Karamese [2], Pinar Bayram [2]*

[1] Kafkas University, Faculty of Medicine, Department of Medical Biochemistry, 36100, Kars, Türkiye
[2] Kafkas University, Faculty of Medicine, Department of Histology and Embryology, 36100, Kars, Türkiye

ARTICLE INFO

Article type:
Original

Article history:
Received: May 20, 2026
Accepted: Jul 26, 2026

Keywords:
Acute kidney injury
Apoptosis
Inflammation
Oxidative stress
Reperfusion injury
Umbelliferone

ABSTRACT

Objective(s): Renal ischemia/reperfusion (IR) injury is a major cause of acute kidney injury, driven by oxidative stress, inflammation, and apoptosis. This study investigated the dose-dependent renoprotective effects of umbelliferone, a coumarin derivative, in a rat model of renal IR injury.

Materials and Methods: Thirty female Wistar rats were randomly assigned to five groups (n=6): Control, Sham, IR, IR+U50 mg/kg, and IR+U100 mg/kg. Serum cytokines (TNF-α, IL-1β, IL-6, IL-10, IL-15, IL-18, TGF-β) were measured by ELISA; renal oxidative stress markers (MDA, GSH, NO) by biochemical assays; NF-κB by immunohistochemistry; and Bax, Bcl-2, NF-κB, NRF2, P2X7, and TNF-α gene expression by RT-qPCR.

Results: IR injury significantly increased pro-inflammatory cytokines, including IL-6 (15.03→25.11 ng/mL), TNF-α (55.63→70.62 ng/l), and IL-1β; elevated MDA (1.90→9.64 nmol/g) and NO (4.02→8.58 μM); and depleted GSH (9.81→1.86 nmol/g) (all $P<0.001$). Renal Bax, NF-κB, P2X7, and TNF-α expression and NF-κB immunoreactivity were increased, whereas NRF2 was decreased ($P<0.001$). Umbelliferone, particularly at 100 mg/kg, significantly reversed these changes, lowering IL-6 (15.12 ng/ml), TNF-α (57.55 ng/l), MDA (3.21 nmol/g), and NO (4.45 μM), restoring GSH (4.27 nmol/g) ($P<0.001$ vs IR), attenuating Bax, NF-κB, P2X7, and TNF-α expression, and partially restoring NRF2.

Conclusion: In this preclinical model, umbelliferone was associated with dose-dependent renoprotective effects against acute renal IR injury, attenuating oxidative stress, inflammation, and apoptosis. Further functional and mechanistic studies are needed before its therapeutic potential can be established.

▶ Please cite this article as:
Baser OF, Guraslan A, Sarikaya BO, Karamese SA, Bayram P. Exploring the renoprotective effects of umbelliferone in rats subjected to ischemia/reperfusion injury. Iran J Basic Med Sci 2026; 29:

Introduction

Acute renal failure is a condition that affects many immune and metabolic events and disrupts the inflammatory-anti-inflammatory balance in the living being (1). The mortality rate is around 10% in hospitalized patients and around 50% in intensive care patients (2). Ischemia initiates a series of biochemical reactions that can lead to cell dysfunction and subsequent cell death by decreasing cellular energy levels and accumulating toxic metabolites in the tissue. In ischemic conditions, the tissue remains hypoxic, and hypoxic tissue damage occurs. As a result of prolonged ischemia, cellular integrity is lost, and cell death occurs (3). Kidneys are among the most damaged organs during reperfusion after ischemia (4). Under normal conditions, there is a balance between free oxygen radicals that damage the cell and anti-oxidant substances that protect the cell. This balance is disrupted after reperfusion of ischemic tissue, shifting in favor of oxidants and leading to acute renal failure (3, 5).

Ischemia/reperfusion (IR) injury is a process characterized by activation of the inflammatory pathway, which results in excessive release of inflammatory agents, apoptosis, and necrosis during recanalization following ischemia and involves reactive oxygen species. IR injury involves many different pathways and mechanisms, including NF-kB transcription, inflammation, oxidative stress, and programmed cell death mechanisms (6-8). Basically, changes in ion concentration in cells lead to an elevation in the level of proinflammatory cytokines and a reduction in the level of anti-oxidant substances. The decrease in anti-oxidant capacity, together with the increase in cytokine levels, renders the cell intolerant to the damage occurring in the reperfusion period (9). Because these processes, oxidative stress, NF-κB-driven inflammation, and apoptosis, are mutually reinforcing rather than independent, therapeutic agents capable of acting simultaneously on multiple arms of this cascade are of particular interest in renal IR injury.

Coumarins are a class of naturally occurring benzopyrone compounds widely distributed in plants and exhibit diverse pharmacological activities, including anti-inflammatory, antimicrobial, antioxidant, and anticancer effects (10). Umbelliferone (7-hydroxycoumarin) is a naturally occurring

***Corresponding author:** Pinar Bayram. Kafkas University, Faculty of Medicine, Department of Histology and Embryology, 36100, Kars, Türkiye. Email: pinarbayram@yandex.com

coumarin derivative widely distributed in medicinal plants and has attracted growing scientific attention for its broad spectrum of pharmacological activities. Multiple studies have demonstrated that umbelliferone exerts beneficial antioxidant, anti-inflammatory, and anti-apoptotic effects, primarily by scavenging reactive oxygen species (ROS) and suppressing key inflammatory mediators such as NF-κB and TLR4 (11, 12). In addition, umbelliferone has been reported to activate the Nrf2/HO-1 anti-oxidant defense pathway, thereby enhancing cellular resilience against oxidative injury (13, 14). Its protective potential has been demonstrated in various models of organ injury, including hepatic ischemia-reperfusion, myocardial ischemia, cerebral ischemia, and acute lung injury (11, 12, 15, 16). Although the protective effects of umbelliferone are well documented in hepatic, myocardial, and cerebral ischemia, as well as in drug-induced nephrotoxicity, its role in renal ischemia-reperfusion injury—particularly its dose-dependent effects and its influence on the P2X7/inflammasome and NRF2 pathways in this specific context—has not yet been clearly established.

The 50 and 100 mg/kg doses were selected based on previous organ-injury studies reporting effective and well-tolerated umbelliferone doses (12), allowing evaluation of a dose-dependent response. The experimental endpoints were chosen to address the three principal and interconnected components of renal IR injury: inflammation (TNF-α, IL-1β, IL-6, IL-15, IL-18, IL-10, TGF-β, NF-κB, and P2X7), oxidative stress (GSH, MDA, NO, and NRF2), and apoptosis (Bax and Bcl-2), together with histopathological assessment. Accordingly, we hypothesized that prophylactic umbelliferone administration would dose-dependently attenuate renal IR injury by suppressing NF-κB–mediated inflammation, reducing oxidative stress and apoptosis, and restoring NRF2-associated anti-oxidant defenses. The present study therefore aimed to determine the dose-dependent renoprotective effects of umbelliferone (50 and 100 mg/kg) in a rat model of renal IR injury and to explore the underlying immunological and molecular mechanisms.

Materials and Methods

Ethical approval and animals

Ethical approval for this research was granted by the Kafkas University Local Committee for Animal Experiments in Kars (Approval No: KAU-HADYEK 2024/131). All interventions involving animals adhered to the ethical regulations established by the institution and national authorities, and were performed in accordance with the European Directive 2010/63/EU, which sets the standards for the care and use of animals in scientific studies.

Thirty female Wistar Albino rats (12 weeks old, 230-250 g) were obtained from the Atatürk University Experimental Research Center. They were housed under standard conditions and fed ad libitum. Animals were randomly assigned to five groups using a simple randomization procedure based on computer-generated random numbers, as shown in Table 1.

Umbelliferone was purchased (MedChem Express, Purity: 99.67% and Cat. No.: HY- N0573) and dissolved in sterile double-distilled water at 50 mg/kg and 100 mg/kg, and administered to rats by intragastric gavage once daily at the same hour for 7 consecutive days (12). The 50 and 100 mg/kg doses were selected based on previous organ-injury studies reporting effective and well-tolerated umbelliferone doses within this range (12), enabling assessment of a dose-dependent response.

Table 1. Experimental groups of ischemia-reperfusion injury model and treatment protocols

No	Group Name	N	Application
1	Control	6	-
2	Sham	6	Only the kidney will be located and then closed
3	Ischemia and Reperfusion	6	Only ischemia and then reperfusion procedure
4	Ischemia-Reperfusion and Umbelliferone 50 mg/kg application	6	UMB at 50 mg/kg by oral gavage for 7 days prior to IR
5	Ischemia-Reperfusion and Umbelliferone 100 mg/kg application	6	UMB at 100 mg/kg by oral gavage for 7 days prior to IR

IR: Ischemia and reperfusion; UMB: umbelliferone

The I/R model will be applied to the animals exactly 24 hours after the 7th day of drug administration. The rats were fasted for 12 hours before the surgery. On the 8th day of the study, all animals were anesthetized with 40 mg/kg ketamine HCl, and a midline abdominal incision of approximately 3 cm was made under sterile conditions. A unilateral renal ischemia model with contralateral nephrectomy was used. First, the left kidney was excised (left nephrectomy) to standardize renal function and to ensure that the assessed outcomes reflected injury to the ischemic kidney. The right renal pedicle was then isolated, and the right renal artery and vein were occluded with a non-traumatic microvascular clamp for 45 min to induce ischemia, which was confirmed by the color change of the kidney. The clamp was subsequently released, and the kidney was reperfused for 3 h; restoration of color confirmed reperfusion. In the Sham group, the same surgical procedure, including laparotomy and isolation of the renal pedicle, was performed without vascular occlusion (17). After the renal capsule was removed, each kidney was divided into two halves. One half was fixed in 10% buffered formalin for 72 hours for histological and immunohistochemical analyses. In contrast, the other half was immediately snap-frozen in liquid nitrogen and stored at -80 ˚C until use for the biochemical and molecular (RT-qPCR) analyses.

Cytokine analysis by ELISA

Blood samples (5 ml) were centrifuged at 4000 rpm for 15 min at 4 ˚C in a refrigerated centrifuge (Beckman Coulter Inc., CA, USA) until a clear supernatant was obtained. The ELISA kits were purchased. Details about the ELISA kits were presented in Table 2. In summary, 100 µl of each standard and sample dilution was added to the appropriate wells and incubated for 90 min at 37 ˚C. 100 µl of Biotinylated Detection Ab working solution was added and incubated for 60 min at 37 ˚C. 100 µl of HRP Conjugate working solution was added and incubated for 30 min at 37 ˚C. 100 µl of Substrate Reagent was added and incubated for 15 min at 37 ˚C in the dark. Until this stage, the plate was washed 3 times with an automated ELISA washer (Biotek ELx50, USA) after each incubation. Finally, 50 µl of Stop Solution was added to each well, and OD values were determined at 450 nm absorbance in the ELISA Reader (Thermo MultiSkan GO, Thermo Fisher Scientific Corporation, MA, USA). All pipetting steps in the study

Table 2. Details about enzyme-linked immunosorbent assay (ELISA) kits

Parameters	Source	Brand	Catalogue No
Interleukin-1-beta	Rat	Feiyue Bio	FY-ER1446
Interleukin -6	Rat	Feiyue Bio	FY-ER5316
Interleukin -10	Rat	Feiyue Bio	FY-ER5319
Interleukin -15	Rat	Feiyue Bio	FY-ER1547
Interleukin -18	Rat	Feiyue Bio	FY-ER1561
Tumor necrosis factor-alpha	Rat	Feiyue Bio	FY-ER1407
Transforming growth factor-beta	Rat	Feiyue Bio	FY-ER5077

were performed using the PRCXI SC9300-V03 automated pipetting robot (PRCXI, Suzhou, China). All standards and samples were assayed in duplicate, and the mean of the two readings was used for analysis.

Biochemical analysis by tissue biochemistry

The kidney tissues were individually pulverized in a mortar with liquid nitrogen. From each rat, 0.025 g of tissue was weighed, and 1.5 ml of buffer solution was added to achieve a 1/60 (w/v) dilution. The homogenates were then homogenized on ice for 10 min using a tissue homogenizer. After filtration through filter paper, the homogenates were centrifuged at 15,000 rpm for 15 min in a refrigerated centrifuge (4 ˚C), and the supernatants were used for analyses. Protein concentrations of the tissue homogenates were determined by the Bradford method, and all biochemical results (NO, MDA, GSH) were normalized to the total protein content of each sample. All samples were processed under identical conditions in a single batch to minimize inter-assay variability, and all measurements were performed in duplicate.

For the determination of nitric oxide (NO), 100 µl of sample was combined with equal volumes of VCl_3 and Griess reagent. After a 30-minute incubation, absorbance was read at 540 nm (17).

Glutathione (GSH) levels were assessed by mixing 200 µl of tissue homogenate with an equal volume of standard solution. The mixture was then supplemented with 1.8 ml of distilled water and 3 ml of precipitating solution, followed by centrifugation at 3000 rpm for 10 min. The supernatant (2 ml) was diluted with 8 ml of PBS, and 1 ml of DTNB was added to initiate the colorimetric reaction. Optical density was recorded at 412 nm (18, 19).

Malondialdehyde (MDA) quantification was performed by adding 0.5 ml of homogenate to 2.5 ml of 20% TCAA. Blank tubes contained only the reagent mixture (3 ml). Both sample and blank tubes received 1 mL of TBA solution and were incubated in a 90 ˚C water bath for 30 min. After incubation, 4 mL of n-butanol was added, and the samples were centrifuged at 3000 rpm for 10 min. The upper organic phase was carefully transferred to clean tubes, and absorbance was measured at 535 nm (18, 19).

Histopathological analysis by immunohistochemistry (IHC)

After the renal capsule was removed, each kidney was divided into two halves; one portion was fixed in 10% buffered formalin for 72 hours. The tissues were then dehydrated through increasing concentrations of ethanol (75% twice for 1 hour; 96% first for 1 hour, then overnight; 100% twice for 1 hour) and embedded in paraffin blocks. Sections were cut at a thickness of 5 µm with a Leica RM2125RT microtome (Leica Microsystems, Wetzlar, Germany). After deparaffinization and rehydration, the slides were stained with hematoxylin and eosin. Histological assessment was performed under a 40× objective by examining approximately ten randomly selected microscopic fields (20, 21).

Immunohistochemical staining was conducted to detect NF-κB p65 expression. Following the clearing steps, the slides were rehydrated through graded alcohols and rinsed in distilled water. To unmask the epitopes masked by formaldehyde, the sections were boiled in citrate buffer solution under high temperature and pressure for 1–2 min. The sections were incubated with a 3% hydrogen peroxide solution in PBS for 10 min. Non-specific binding sites were blocked using a protein block applied for 5 min. Excess blocking reagent was removed, and the tissues were incubated overnight at 4 ˚C with a monoclonal anti-NF-κB primary antibody (1:100, Santa Cruz Biotechnology, sc-8008). The following day, the slides were washed with PBS, treated with a biotinylated secondary antibody for 10 min, and then incubated with streptavidin-peroxidase. Signal visualization was achieved using DAB chromogen. Mayer's hematoxylin was used as a counterstain, and the slides were then mounted with Entellan. Prepared sections were examined under an Olympus CX41 light microscope (20, 21). Negative controls were prepared by omitting the primary antibody and incubating sections with antibody diluent alone, under otherwise identical conditions.

NF-κB p65 immunoreactivity was evaluated semi-quantitatively. For each animal, randomly selected, non-overlapping cortical fields were examined at ×40 magnification, and the proportion of NF-κB–positive tubular cells was scored on a 0-3 scale (0: <5% positive cells; 1: 5-25%; 2: 26-50%; 3: >50%). Scoring was performed independently by two observers blinded to group allocation, and the mean score per group was used for analysis.

Molecular analysis by real-time PCR

Total RNA was isolated from the snap-frozen, non-fixed kidney tissue stored at -80 ˚C. Total RNA was isolated from kidney tissue to determine the expression levels of Bax, BcL-2, NF-kB, NRF2, P2X7, and TNF-alpha genes. According to the Ecotech Total RNA Isolation Kit protocol (Cat. No: E2075, Erzurum, Türkiye), binding buffer was added, and the samples were loaded onto the spin column. DNase was then applied to the column and incubated for 15 min to prevent DNA contamination. The column was subsequently washed with the provided wash buffers, and RNA was eluted with 30 µl of elution buffer. Following isolation, RNA concentrations and purity were measured using the Thermo Scientific MultiSkan GO. For optimization purposes, all RNA samples were diluted with the kit's elution buffer to a final concentration of 100 ng/µl. All pipetting steps in the study were performed using the PRCXI SC9300-V03 automated pipetting robot (PRCXI, Suzhou, China). For cDNA synthesis, EcoScript 5x First Strand cDNA Synthesis Kit (Cat. No: ERT200, Erzurum, Türkiye) was used according to the manufacturer's instructions. The amounts and setup of the reaction mixture recommended in the EcoScript 5x First Strand cDNA Synthesis Kit are presented in Table 3.

The mRNA expression levels of Actb (housekeeping gene), Bax, Bcl-2, NF-κB, NRF2, P2X7, and TNF-α genes in

Table 3. Recommended reaction mixture volumes and setup for cDNA synthesis

	Component	Amount		Temperature	Time
Preparation of the reaction mixture	cDNA Synthesis Kit	4 µl	Reaction Setup	42 ˚C	120 min
	Total RNA	1 µl		85 ˚C	5 min
	ddH2O	15 µl		4 ˚C	∞

cDNA samples derived from kidney tissue were quantified using the SYBR Green Gene Expression Master Mix Kit (Table 4).

Amplification and quantification were performed on a Qiagen Rotor-Gene Q 5-plex HRM Real-Time PCR System (Qiagen, Hilden, Germany). Ct (threshold cycle) values were automatically converted by the instrument using the $2^{\Delta\Delta}$Ct method, and the results were expressed as $\log_2$ (fold change) for gene expression analysis. The Control group was used as the calibrator, and the expression of each target gene was normalized to Actb and expressed relative to the Control group using the 2^-ΔΔCt method. Amplification specificity was confirmed by melt-curve analysis at the end of each run, which yielded a single peak for every primer pair, indicating the absence of primer dimers and non-specific products. Primer amplification efficiencies were determined from standard curves generated by serial dilutions of pooled cDNA. They were within the acceptable range of 90-110% for all genes, confirming comparable efficiencies between the target and reference genes, as required for the 2^-ΔΔCt method. The forward and reverse primer sequences are shown in Table 5 (22, 23).

All outcome assessments (histopathological and immunohistochemical scoring, ELISA measurements, and RT-qPCR analyses) were performed by investigators blinded to group allocation.

Statistical analysis

All data are expressed as mean±standard deviation (SD). Statistical analyses were performed using GraphPad Prism 10.1. The normality of the data was assessed using the Shapiro–Wilk test, and homogeneity of variances was evaluated using the Brown-Forsythe test. As the data met these assumptions, group comparisons were performed using one-way ANOVA followed by Tukey's multiple comparisons test, which inherently corrects for multiple pairwise comparisons. Results are reported as mean±SD together with the corresponding p-values. A p-value<0.05 was considered statistically significant.

Results

Systemic cytokine levels were quantified by ELISA to evaluate the inflammatory response to renal IR injury and the potential role of umbelliferone, and distinct alterations were observed across pro- and anti-inflammatory mediators. IL-15 (Figure 1A) was elevated in the IR group (20.07 ng/l) relative to the control (15.50 ng/l) and sham (15.25 ng/l) groups, and both umbelliferone doses significantly lowered IL-15 (IR+U50: 16.19 ng/l; IR+U100: 14.95 ng/l). IL-10 (Figure 1B) was highest in the control group (73.84 pg/ml) and significantly lower in the IR group (53.60 pg/ml, versus control); umbelliferone did not significantly restore IL-10 (IR+U50: 61.78 pg/ml; IR+U100: 55.53 pg/ml). IL-18 (Figure 1C) increased progressively, from 52.45 pg/ml in the control group to 94.37 pg/ml in the IR group, and remained elevated after treatment (IR+U50: 119.19 pg/ml; IR+U100: 118.33 pg/ml), reaching significance for IR+U50 versus control. Notably, unlike the other cytokines assessed, IL-18 did not decrease with umbelliferone treatment; instead, it remained elevated—and numerically higher than the IR group, indicating a response pattern distinct from the other inflammatory mediators. TGF-β (Figure 1D)

Table 5. Forward and reverse primers of genes Bax, BcL-2, NF-kB, NRF2, P2X7 and TNF-alpha, used to evaluate levels of apoptosis and inflammation

Genes	Primers
Actb	F: 5'- CAGCCTTCCTTCTTGGGTATG-3' R: 5'- AGCTCAGTAACAGTCCGCCT-3'
Bax	F: 5'- TGCAGAGGATGATTGCTGAC-3' R: 5'- GATCAGCTCGGGCACTTTAG-3'
BcL-2	F: 5'- ATGGACT[illegible]CCGGTCGCCACC-3' R: 5'- GGGCTGTC[illegible]CGGCAGCCGCC-3'
NF-kB	F: 5'-CTCC[illegible]GGCAGCATCC-3' R: 5'-AGCCGC[illegible]CAGCATTCAGGTCGTAG-3'
NRF2	F: 5′-[illegible]ACAC[illegible]GTCCACAGCTCATC-3′ R: 5′-TG[illegible]ATCAAATCCATGTCCTG-3′
P2X7	F: 5'-[illegible]GGTGGATTCTGGAAGGCTC-3' R: 5'- GCTGATGCTGTGGGTTTGTT-3'
TNF-alpha	F: 5′-CTCTCTCTAATCAGCCCTCTG-3′ R: 5′-GAGGACCTGGGAGTAGATGAG-3′

Table 4. Recommended reaction mixture volumes and setup for SYBR green master mix refers to a commercially purchased, ready-to-use reaction mixture

	Component	Amount		Temperature	Time
Preparation of the reaction mixture	2x SYBR Master Mix	10 µl	Reaction Setup	95 ˚C	2 min
	Forward Primer	0,5 µl		95 ˚C	10 sec
	Reverse Primer	0,5 µl		60 ˚C	30 sec
	Template cDNA	1 µl		40 cycles	
	ddH2O	8 µl			

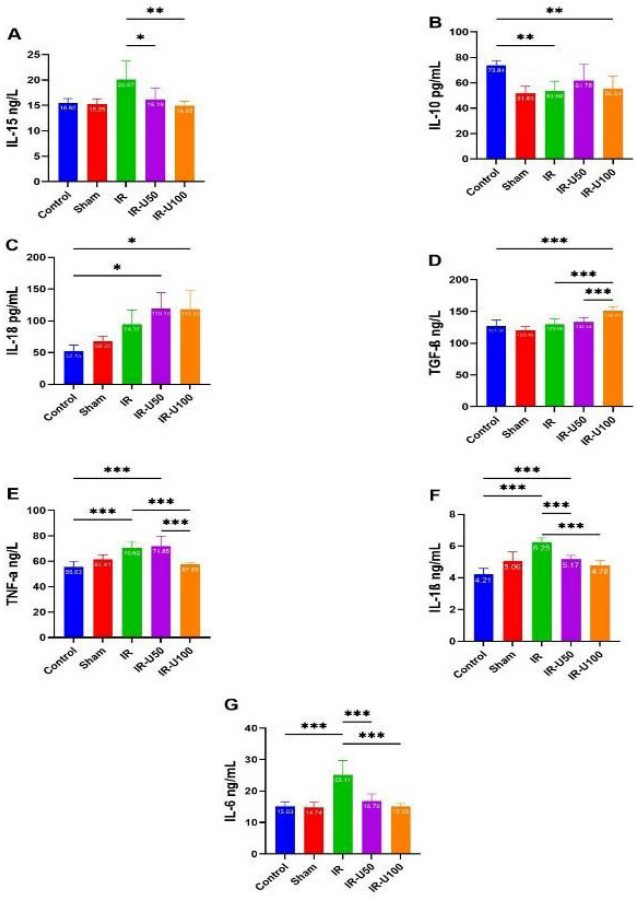

Figure 1. Rat systemic cytokine levels measured by enzyme-linked immunosorbent assay (ELISA) in the experimental groups: interleukin-15 (IL-15), interleukin-10 (IL-10), interleukin-18 (IL-18), transforming growth factor-beta (TGF-β), tumor necrosis factor-alpha (TNF-α), interleukin-1 beta (IL-1β), and interleukin-6 (IL-6)

Data are presented as mean±standard deviation (SD). Statistical analysis was performed using one-way analysis of variance (ANOVA) followed by Tukey's *post hoc* test. *significant versus the Control group; +significant versus the ischemia-reperfusion (IR) group; #significant between the two umbelliferone (U) doses (IR-U50 vs IR-U100). *P<0.05, **P<0.01, ***P<0.001

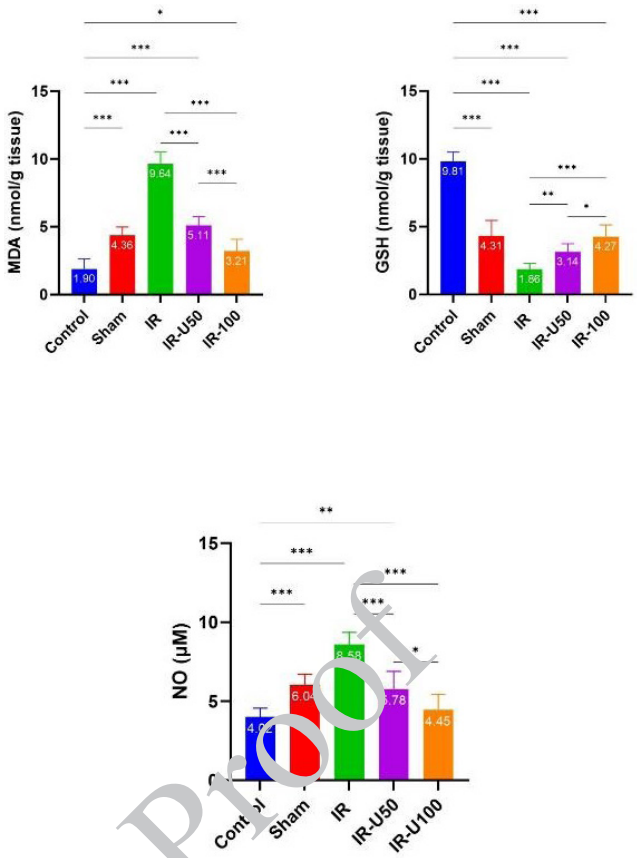

Figure 2. Oxidative stress markers in the rat experimental groups: Malondialdehyde (MDA), glutathione (GSH), and nitric oxide (NO)

Data are presented as mean±standard deviation (SD). Statistical comparisons were performed using one-way analysis of variance (ANOVA) followed by Tukey's *post hoc* test. Horizontal bars denote the compared groups, including each group versus the control group, versus the ischemia-reperfusion (IR) group, and the comparison between the two umbelliferone (U) doses (IR-U50 vs IR-U100). *P<0.05, **P<0.01, ***P<0.001

was comparable among the control, sham, IR, and IR+U50 groups (≈120–133 ng/l), whereas the IR+U100 group showed a significant increase (150.91 ng/l) versus both the IR and IR+U50 groups. TNF-α (Figure 1E) was significantly elevated in the IR group (70.62 ng/l) compared with the control group (55.63 ng/l) and remained high in the IR+U50 group (71.85 ng/l, versus control). In contrast, the higher dose significantly reduced TNF-α to near-control levels (57.55 ng/l). IL-1β (Figure 1F) was significantly increased in the IR group (6.25 ng/ml) relative to control (4.21 ng/ml), and both umbelliferone doses significantly reduced it versus the IR group (IR+U50: 5.17 ng/ml; IR+U100: 4.78 ng/ml). Finally, IL-6 (Figure 1G) showed the most pronounced response, increasing markedly in the IR group (25.11 ng/ml) versus control (15.03 ng/ml); both doses significantly suppressed IL-6 (IR+U50: 16.78 ng/ml; IR+U100: 15.12 ng/ml), with IR+U100 restoring levels close to baseline.

Oxidative stress was assessed by measuring GSH, MDA, and NO levels across the experimental groups (Figure 2). GSH, reflecting anti-oxidant capacity, was markedly depleted by IR injury, decreasing from 9.81 nmol/g tissue in the control group to 1.86 nmol/g tissue in the IR group (P<0.001). Both umbelliferone doses partially restored GSH in a dose-dependent manner (IR+U50: 3.14 nmol/g tissue, P<0.01; IR+U100: 4.27 nmol/g tissue, P<0.001; both versus IR), with the higher dose being significantly more effective than the lower dose (P<0.05). Conversely, MDA, an indicator of lipid peroxidation, was markedly elevated in the IR group (9.64 nmol/g tissue) compared with the control group (1.90 nmol/g tissue, P<0.001). Both doses significantly reduced MDA relative to IR (IR+U50: 5.11 nmol/g tissue; IR+U100: 3.21 nmol/g tissue; both P<0.001), and the reduction was significantly greater at the higher dose (IR+U50 vs IR+U100, P<0.001). Similarly, NO was significantly increased following IR injury (8.58 µM versus 4.02 µM in the control group, P<0.001), and both umbelliferone doses significantly suppressed NO production relative to IR (IR+U50: 5.78 µM; IR+U100: 4.45 µM; both P<0.001), with a further significant decrease at the higher dose (IR+U50 vs IR+U100, P<0.05), returning NO toward control levels.

When the kidney tissue was examined for histopathological analysis, all structures such as vessels, glomeruli, and proximal and distal tubules were evaluated as normal in the control and sham surgery groups (Figure 3A, B). The histopathological changes determined in the IR group were impaired tubules, lymphocyte infiltration, cellular swelling, and damaged glomeruli (Figure 3C). On the other hand, when the IR+U50 and IR+U100 groups were examined, the most promising results were observed

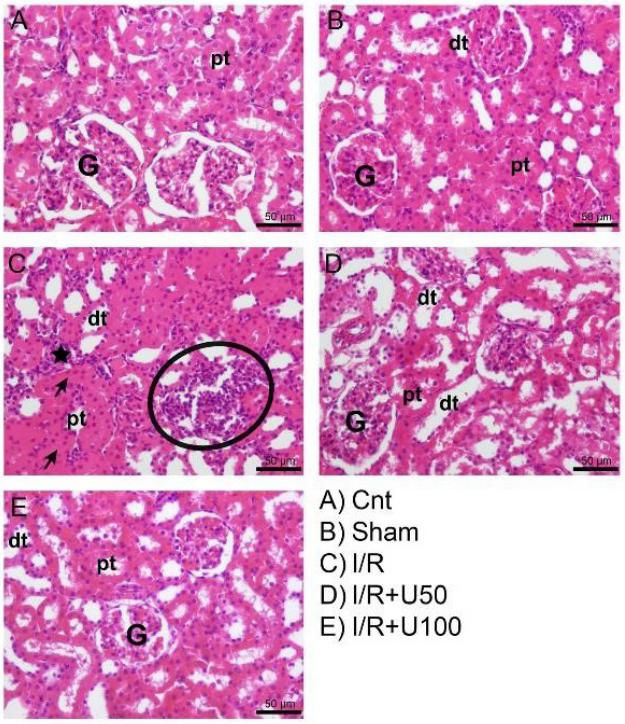

Figure 3. Histological examination of rat kidney tissue
(A) Control (Cnt), (B) Sham, (C) ischemia-reperfusion (I/R), (D) I/R+umbelliferone 50 mg/kg (I/R+U50), (E) I/R+umbelliferone 100 mg/kg (I/R+U100). G: renal glomerulus; pt: proximal tubule; dt: distal tubule; circled area: damaged renal glomerulus; star: lymphocyte infiltration; arrow: cellular swelling. Staining: hematoxylin and eosin (H&E). Scale bar: 50 µm

in the IR+U100 group. The glomeruli and proximal and distal tubules had a healthier appearance than the IR group (Figure 3E). It was determined that leukocyte infiltration decreased in both doses (Figure 3D, E).

Kidney sections from all groups were labeled with an anti-NF-κB primary antibody for immunohistochemical analysis. In the sham and control groups, a few NF-κB-positive cells were observed in the tubules. In the IR group, many positive cells were detected, especially in the tubules. The number of immunopositive cells, particularly in the tubules, in the IR+U50 group was similar to that in the IR group; however, the immunopositive cell density in the IR+U100 group decreased compared to the ischemia group (Figure 4).

qPCR analysis revealed that the expression levels of pro-apoptotic Bax and the inflammatory mediators NF-κB, P2X7, and TNF-α were significantly increased in the IR group (P<0.001). In contrast, no significant change was observed in the expression of the anti-apoptotic Bcl-2. These alterations suggest that cellular stress, inflammation, and apoptosis are simultaneously activated during the reperfusion phase. Administration of both U50 and U100 was associated with reduced IR-induced elevations of Bax, NF-κB, P2X7, and TNF-α expression, consistent with attenuated pro-inflammatory and pro-apoptotic gene expression profiles. This effect supports umbelliferone's potential to attenuate cell death and modulate inflammatory pathways. In addition, the decrease in NRF2 expression in the IR group indicates suppression of the oxidative stress response, whereas umbelliferone partially restored NRF2 levels, suggesting reactivation of anti-oxidant defense mechanisms. The expression levels of related genes are shown in Figure 5.

Renal ischemia-reperfusion injury is a major contributor to acute kidney failure and is commonly encountered in clinical settings such as surgical operations and kidney transplant procedures. It is characterized by reduced oxygen and nutrient delivery during ischemia, increased ROS generation upon reperfusion, and activation of inflammatory pathways. Over time, this sequence can impair renal function and may progress to chronic kidney disease (24, 25).

The present study provides a multidimensional evaluation of the pathophysiological events triggered by renal IR injury. It indicates that umbelliferone is associated with renoprotective effects, accompanied by modulation of oxidative stress, inflammation, and apoptosis. The pattern observed here suggests that these processes may be engaged in parallel rather than sequentially during reperfusion.

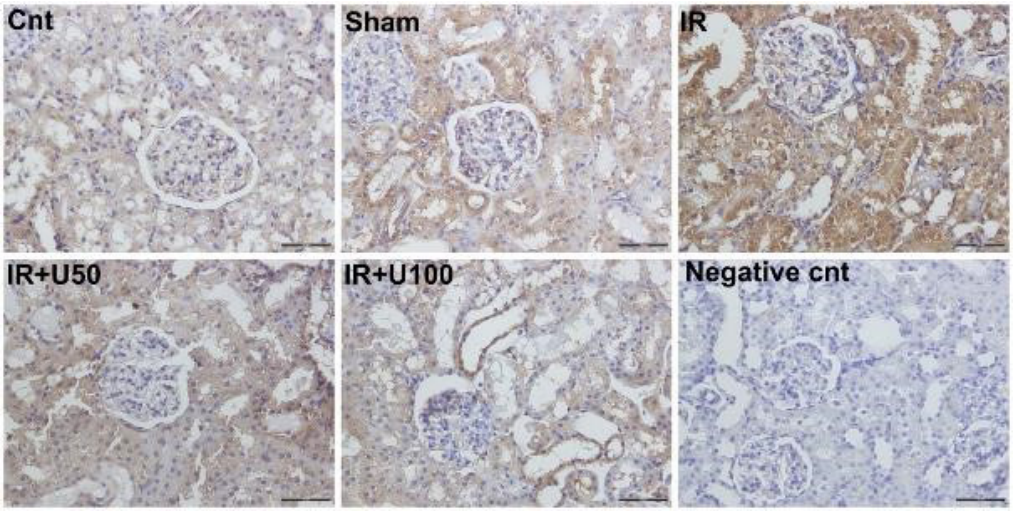

Figure 4. Nuclear factor kappa B (NF-κB)-labeled cells in kidney tissue of all rat experimental groups: Control (Cnt), Sham, ischemia-reperfusion (IR), IR+umbelliferone 50 mg/kg (IR+U50), IR+umbelliferone 100 mg/kg (IR+U100), and negative control
Brown areas indicate positive immunostaining for the anti-NF-κB primary antibody. Scale bar: 50 µm

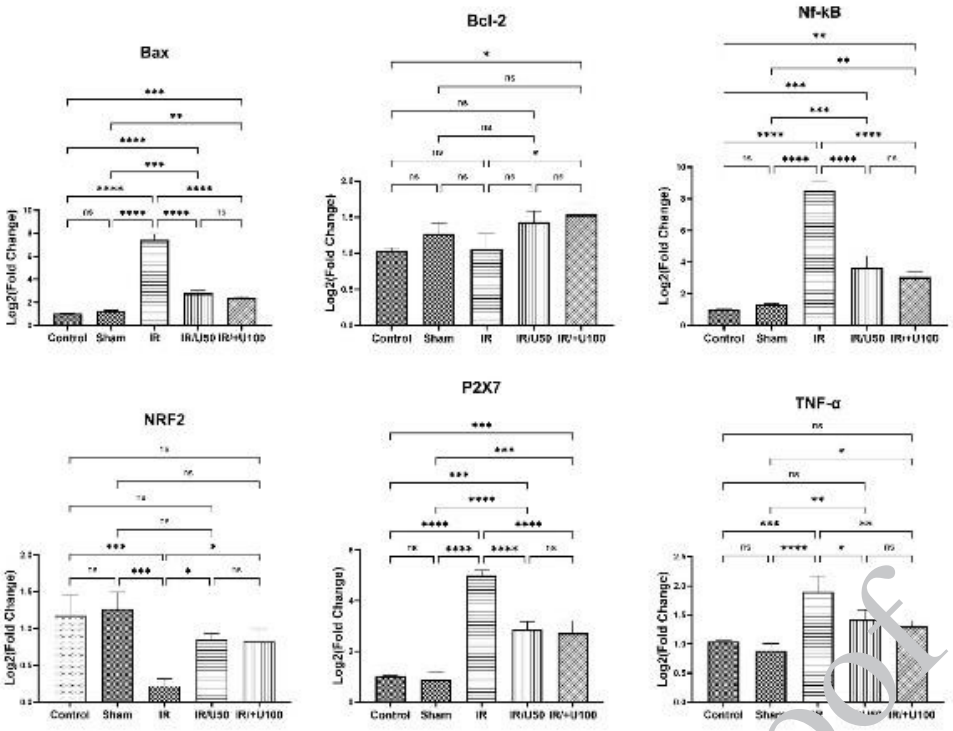

Figure 5. Relative mRNA expression levels of Bcl-2-associated X protein (Bax), B-cell lymphoma 2 (Bcl-2), nuclear factor kappa B (NF-κB), nuclear factor erythroid 2-related factor 2 (NRF2), purinergic receptor P2X7 (P2X7), and tumor necrosis factor alpha (TNF-α) in the experimental rat groups, expressed as log2(fold change)

Data are presented as mean±SD. Statistical analysis was performed using one-way analysis of variance (ANOVA) with Tukey's *post hoc* test. ns: not significant; $^{*}P<0.05$, $^{**}P<0.01$, $^{***}P<0.001$, $^{****}P<0.0001$

Collectively, these events compromise renal structural and functional integrity. These results support earlier findings in the literature indicating that reperfusion, more than ischemia alone, is the main cause of renal cell injury because it triggers excessive ROS production, activates inflammatory pathways, and contributes to increased cell death by necrotic, necroptotic, apoptotic, and autophagic mechanisms (26, 27).

One of the major findings of this experimental study is the strong activation of NF-κB signaling in the IR group. NF-κB is a major transcription factor that drives the inflammatory response during IR, and it is usually activated through ROS-dependent IκBα degradation, TLR stimulation, and mitochondrial dysfunction (28). Rather than merely confirming these elevations, the co-occurrence of increased NF-κB with raised TNF-α, IL-1β, IL-6, and P2X7 may suggest that IR engaged a coordinated NF-κB-dependent transcriptional program rather than isolated cytokine release. Importantly, P2X7 is one of the major drivers of inflammasome-related pathways and is known to induce NLRP3 activation, caspase-1 cleavage, and the release of some inflammation-related cytokines (29). According to the obtained data, the simultaneous increases in NF-κB and P2X7 may support the possibility that IR initiates cytokine-mediated inflammatory cell death pathways.

Umbelliferone treatment (especially 100 mg/kg) was associated with significantly lower levels of these inflammatory mediators. Additionally, the reduction in NF-κB immunoreactivity is consistent with this molecular finding. Yan *et al.* reported that umbelliferone treatment significantly suppressed NF-κB levels (30). Similarly, Ali *et al* reported that umbelliferone application at 30 mg/kg/day for 14 days resulted in a dramatic decline in the total and nuclear NF-κB expression (14). The decrease in P2X7 expression also suggests that umbelliferone may interfere with ATP-mediated inflammasome activation, a mechanism that may contribute to its anti-inflammatory efficacy. Although the literature on this topic is limited, a study reported that umbelliferone reduced P2X7 levels by inhibiting TXNIP in relation to NLRP3 activation (31).

Oxidative stress plays a key role in the development of renal IR injury. Beyond reflecting lipid peroxidation (MDA) and anti-oxidant depletion (GSH), this oxidative shift may be upstream of the inflammatory response, since ROS have been reported to promote IκBα degradation and NF-κB activation while impairing NRF2 signaling—linking the oxidative and inflammatory findings of this study within a single redox-sensitive axis. During reperfusion, excessive ROS can damage mitochondrial membranes, cause DNA injury, and activate redox-sensitive inflammatory factors, which together promote both apoptotic and necrotic cell death (26). Umbelliferone significantly increased GSH levels and reduced MDA and NO concentrations, consistent with potent anti-oxidant effects. Research from Türkiye has revealed that umbelliferone behaves as a ROS scavenger in the IR process in kidney, heart, and lung tissues by reducing SOD and GSH levels and increasing MDA and MPO levels (32). Another investigation demonstrated that umbelliferone markedly increased GSH levels and enhanced the activities of GST and SOD enzymes, while substantially lowering renal MDA concentrations relative to the IR group (14). Yan *et al* also reported that 20 mg/kg umbelliferone application caused a decrease in the levels of LPO and an increase in the levels of CAT, SOD, and GPx (30). The data

from the literature are consistent with our study.

NRF2 regulation in our study highlights the anti-oxidant role of umbelliferone. NRF2 is a master transcription factor controlling cellular detoxification and anti-oxidant pathways (33). The NRF2 down-regulation observed in the IR group is consistent with studies showing that excessive ROS can suppress NRF2 nuclear localization and impair anti-oxidant gene transcription (13, 14).

The apoptosis results also support the renoprotective effects of umbelliferone. IR-induced Bax up-regulation may be associated with activation of the intrinsic mitochondrial pathway of apoptosis. The lack of significant change in Bcl-2 expression suggests that the pro-apoptotic shift is primarily driven by Bax elevation rather than suppression of anti-apoptotic regulators. The reduction in Bax expression observed with umbelliferone is consistent with decreased activation of the intrinsic apoptotic pathway, although mitochondrial integrity was not directly assessed. Previous studies have attributed this anti-apoptotic effect to umbelliferone and reported that umbelliferone treatment restored the levels of apoptosis parameters (30). An unexpected finding was that IL-18 did not decrease with umbelliferone treatment, unlike the other cytokines assessed; instead, it remained elevated at both doses. This may reflect the distinct regulation of IL-18, which depends primarily on caspase-1/inflammasome processing rather than direct NF-κB-driven transcription, and may therefore follow different kinetics than the other mediators examined within the single 3-hour reperfusion window used here.

Considered together, these findings outline an integrated, self-amplifying injury network rather than a set of independent events: reperfusion-derived ROS may both contribute to IκBα degradation and be associated with NF-κB and suppress NRF2-driven anti-oxidant transcription. At the same time, NF-κB and P2X7 may reinforce one another through cytokine release and inflammasome priming, and the resulting oxidative–inflammatory milieu may shift the Bax/Bcl-2 balance toward intrinsic apoptosis. Within this framework, the concurrent attenuation of NF-κB, P2X7, TNF-α, IL-1β, and IL-6, the partial recovery of NRF2, the reduction in Bax, and the preserved tubular architecture suggest that umbelliferone acts at the convergence point of the oxidative and inflammatory arms of IR injury rather than on a single isolated target—consistent with the multi-target profile expected of a coumarin derivative. This interpretation also helps account for the dose-dependent response, in which the higher dose more effectively interrupts this mutually reinforcing loop.

Histopathological analysis provides structural support for biochemical and molecular findings. In the IR group, excessive tubular degeneration, glomerular disruption, interstitial edema, and leukocyte infiltration were observed in our study. These alterations reflect the complex interplay of oxidative stress, endothelial injury, and inflammation and are characteristic of renal IR injury. Both umbelliferone doses alleviated these structural abnormalities. Studies on the same issue reported that the pathological changes of kidneys because of IR were reduced by umbelliferone application, as evidenced by slight vacuolation of epithelial cells in the epithelial lining of certain renal tubules and minimal congestion of the glomerular tuft (14, 34).

This study has several limitations that should be acknowledged. First, only a single, relatively short reperfusion period (3 hours) was evaluated; therefore, the present findings reflect the acute phase of injury and do not capture longer-term outcomes such as functional recovery, interstitial fibrosis, or progression toward chronic kidney disease. Second, renal injury was assessed using histological, immunohistochemical, biochemical, and molecular endpoints, whereas conventional functional markers of renal injury, such as serum creatinine and blood urea nitrogen, were not measured. Third, the molecular alterations were demonstrated mainly at the transcriptional level, and protein-level confirmation was limited to NF-κB; validation of the remaining targets by additional protein-based methods, such as Western blotting, was not performed. Future studies addressing these aspects are warranted to establish the renoprotective potential of umbelliferone further.

Conclusion

In this experimental rat model, umbelliferone was associated with modulation of several pathways involved in renal IR injury, including oxidative stress, inflammation, and apoptosis. These effects were accompanied by reduced NF-κB immunoreactivity, decreased expression of Bax, NF-κB, P2X7, and TNF-α, partial restoration of NRF2 expression, lower oxidative stress markers, and attenuation of tubular and glomerular damage. Together, these findings suggest that umbelliferone may exert renoprotective effects against acute renal IR injury in this preclinical model. However, these conclusions are limited by the single, short reperfusion period and the use of expression- and tissue-based endpoints without functional renal markers; accordingly, they should be interpreted with caution and should not be extrapolated to clinical or therapeutic use in humans at this stage. Further studies, including functional and long-term assessments, protein-level mechanistic confirmation, and evaluation in additional models, are required before the therapeutic potential of umbelliferone in renal IR injury can be established.

Acknowledgment

This research has been supported by Kafkas University Scientific Research Projects Coordination Unit (Project Number: 2025-TS-44).

Data Availability Statement

The data used in this study are available from the corresponding author upon reasonable request.

Ethics Approval Statement

This study was approved by the Local Ethics Committee for Animal Experiments of Kafkas University, Türkiye (Approval No: KAÜ-HADYEK/2024-131).

Authors' Contributions

P B and OF B conceived the research and drafted the primary manuscript. OF B carried out the biochemical analyses and PCR experiments. BO S and A G conducted histological staining. SA K and P B performed the ELISA tests and interpreted the results. All authors reviewed and approved the final manuscript.

Conflicts of Interest

All authors confirm they have no conflicts of interest.

Declaration

During the preparation of this manuscript, the authors used AI (Claude) solely to improve the language and readability of the text.

References

1. Shiva N, Sharma N, Kulkarni YA, Mulay SR, Gaikwad AB. Renal ischemia/reperfusion injury: An insight on *in vitro* and *in vivo* models. Life Sci 2020; 256: 117860.
2. Beker BM, Corleto MG, Fieiras C, Musso CG. Novel acute kidney injury biomarkers: Their characteristics, utility and concerns. Int Urol Nephrol 2018; 50: 705-713.
3. Ozan E, Koyutürk L, Sapmaz T. Böbrek iskemi-reperfüzyon hasarında antioksidan olarak prostoglandin E1 (pgE1) kullanımının incelenmesi: Deneysel çalışma. Fırat Tıp Dergisi 2004; 9: 67-71.
4. Zhou T, Prather ER, Garrison DE, Zuo L. Interplay between ROS and antioxidants during ischemia-reperfusion injuries in cardiac and skeletal muscle. Int J Mol Sci 2018; 19: 417.
5. Saylan A, Firat T, Yis OM, Dede G, Carver H. Analysis of antioxidant effects of lycopene and caffeine in experimentally induced renal ischemia-reperfusion injury in rats. J Harran Univ Facult 2021; 18; 510-516.
6. Karamese SA, Toktay E, Unal D, Selli J, Karamese M, Malkoc I. The protective effects of beta-carotene against ischemia/reperfusion injury in rat ovarian tissue. Acta Histochem 2015; 117: 790-797.
7. Gottlieb RA. Cell death pathways in acute ischemia/reperfusion injury. J Cardiovasc Pharmacol Ther 2011; 16: 233-238.
8. Kanduc D, Mittelman A, Serpico R, Sinigaglia E, Sinha AA, Natale C, *et al.* Cell death: Apoptosis versus necrosis (review). Int J Oncol 2002; 21: 165-170.
9. Şener G, Yeğen BÇ. İskemi reperfüzyon hasarı. Klinik Gelişim Dergisi 2009; 22: 5-13.
10. Karamese M, Erol HS, Albayrak M, Guvendi GF, Aydin E, Karamese SA. Antioxidant and anti-inflammatory effects of apigenin in a rat model of sepsis: An immunological, biochemical, and histopathological study. Immunopharmacol Immunotoxicol 2016; 38: 228-237.
11. Hassanein EHM, Khader HF, Elmansy A, Seleem HS, Elfiky M, Mohammedsaleh ZM, *et al.* Umbelliferone alleviates hepatic ischemia/reperfusion-induced oxidative stress injury via targeting Keap-1/Nrf-2/ARE and TLR4/NF-kappaB-p65 signaling pathway. Environ Sci Pollut Res Int 2021; 28: 67863-67879.
12. Bati YU, Sezer M, Yilmaz A, Baser L, Guraslan A, Bayram P, *et al.* The Protective effects of dose-dependent umbelliferone application on CLP-induced acute lung injury (ALI) model. J Biochem Mol Toxicol 2025; 39: e70549.
13. Yang Z, Ning R, Liu Q, Zang R, Liu S, Sun S. Umbelliferone attenuates cisplatin-induced acute kidney injury by inhibiting oxidative stress and inflammation via NRF2. Physiol Rep 2023; 11: e15879.
14. Ali FE, Hassanein EH, El-Bahrawy AH, Omar ZMM, Rashwan EK, Abdel-Wahab BA, *et al.* Nephroprotective effect of umbelliferone against cisplatin-induced kidney damage is mediated by regulation of NRF2, cytoglobin, SIRT1/FOXO-3, and NF-kB-p65 signaling pathways. J Biochem Mol Toxicol 2021; 35: e22738.
15. Gan J, Qian W, Lin S. Umbelliferone alleviates myocardial ischemia: The role of inflammation and apoptosis. Inflammation 2018; 41: 464-473.
16. Wang X, Li R, Wang X, Fu Q, Ma S. Umbelliferone ameliorates cerebral ischemia-reperfusion injury via upregulating the PPAR gamma expression and suppressing TXNIP/NLRP3 inflammasome. Neurosci Lett 2015; 600: 182-187.
17. Can I, Guraslan A, Baser OF, Yıldız GN, Toplaoglu I, Karamese SA, *et al.* The protective effects of a single dose myricetin application on CLP-induced rat sepsis model by analyzing some immune mechanisms. Immunopharmacol Immunotoxicol 2025; 47: 305-316.
18. Baser OF, Karapehlivan M, Kukurt A, Uysal AY, Kafkas E, Dağ S, *et al.* Protective effect of boric acid against 3-NPA-induced ovarian damage. Biol Trace Elem Res 2026; 204: 1008-1021.
19. Cumaoglu MO, Makav M, Dag S, *et al.* Combating oxidative stress and inflammation in gentamicin-induced nephrotoxicity using hydrogen-rich water. Tissue Cell 2024; 91: 102604.
20. Bayram P, Aksak Karamese S, Ozdemir B, Salum C, Erol HS, Karamese M. Two flavonoids, baicalein and naringin, are effective as anti-inflammatory and antioxidant agents in a rat model of polymicrobial sepsis. Immunopharmacol Immunotoxicol 2023; 45: 597-606.
21. Karamese M, Aydin H, Gelen V, Sengul E, Karamese SA. The anti-inflammatory, antioxidant and protective effects of a probiotic mixture on organ toxicity in rat model. Future Microbiol 2020; 15: 401-412.
22. Dai C, Li B, Zhou Y, Li D, Zhang S, Li H, *et al.* Curcumin attenuates quinocetone induced apoptosis and inflammation via the opposite modulation of Nrf2/HO-1 and NF-kB pathway in human hepatocyte L02 cells. Food Chem Toxicol 2016; 95: 52-63.
23. Sul OJ, Ra SW. Quercetin prevents LPS-induced oxidative stress and inflammation by modulating NOX2/ROS/NF-kB in lung epithelial cells. Molecules 2021; 26: 6949.
24. Chen CC, Chapman WC, Hanto DW. Ischemia-reperfusion injury in kidney transplantation. Front Biosci 2015; 7: 117-134.
25. Rodriguez F, Bonacasa B, Fenoy FJ, Salom MG. Reactive oxygen and nitrogen species in the renal ischemia/reperfusion injury. Curr Pharm Des 2013; 19: 2776-2794.
26. Kalogeris T, Baines CP, Krenz M, Korthuis RJ. Cell biology of ischemia/reperfusion injury. Int Rev Cell Mol Biol 2012; 298: 229-317.
27. Zuk A, Bonventre JV. Acute kidney injury. Annu Rev Med 2016; 67: 293-307.
28. Liu T, Zhang L, Joo D, Sun S-C. NF-κB signaling in inflammation. Signal Transduct Target Ther 2017; 2: 1-9.
29. Di Virgilio F, Dal Ben D, Sarti AC, Giuliani AL, Falzoni S. The P2X7 receptor in infection and inflammation. Immunity 2017; 47: 15-31.
30. Yan R, Yang H, Jiang X, Lai X. Renal protective effect of umbelliferone on acute kidney injury in rats via alteration of HO-1/Nrf2 and NF-κB signaling pathway. Dokl Biochem Biophys 2024; 518: 442-451.
31. Dutartre P. Inflammasomes and natural ingredients towards new anti-inflammatory agents. Molecules 2016; 21: 1492.
32. Icoglu Aksakal F, Koc K, Geyikoglu F, Karakaya S. Ameliorative effect of umbelliferone in remote organ injury induced by renal ischemia-reperfusion in rats. J Food Biochem 2021; 45: e13628.
33. Hammad M, Raftari M, Cesario R, *et al.* Roles of oxidative stress and Nrf2 signaling in pathogenic and non-pathogenic cells: A possible general mechanism of resistance to therapy. Antioxidants 2023; 12: 1371.
34. Hassanein EH, Mohamed WR, Shalkami A-GS, Khalaf MM, Hemeida RAM. Renoprotective effects of umbelliferone on methotrexate-induced renal injury through regulation of Nrf-2/Keap-1, P38MAPK/NF-κB, and apoptosis signaling pathways. Food Chem Toxicol 2018; 116: 152-160.